

## Research Article

# Synthesis and Characterization of Activated Carbons Prepared from Agro-Wastes by Chemical Activation

Joel Brian Njewa , Ephraim Vunain , and Timothy Biswick

University of Malawi, Chemistry Department, P.O. Box 280, Zomba, Malawi

Correspondence should be addressed to Joel Brian Njewa; njewajoel@gmail.com

Received 11 December 2021; Revised 13 February 2022; Accepted 9 March 2022; Published 22 March 2022

Academic Editor: Wenshan Guo

Copyright © 2022 Joel Brian Njewa et al. This is an open access article distributed under the Creative Commons Attribution License, which permits unrestricted use, distribution, and reproduction in any medium, provided the original work is properly cited.

In this present study, activated carbons were prepared from rice husks and potato peels by chemical activation with 40% phosphoric acid ( $H_3PO_4$ ). The effects of carbonization temperature and impregnation ratio were investigated with a continuous activation period. Physicochemical characteristics such as surface morphology, surface charge, and surface functional groups were assessed. According to X-ray diffraction measurements, the results showed that the activated carbons had identical pH<sub>pzc</sub> (6.8) and that the activated carbons generated were carbonaceous. The existence of hydroxyl, carbonyl, amines, aromatic, and other functional groups, which are excellent for adsorption, was revealed by surface chemistry studies. Micrographs taken with a scanning electron microscope indicated wide opening pores with a larger mesoporous surface area and many linked pores. Rice husk activated carbon outperformed potato peel activated carbon in laboratory tests. The research has shown that the agro-wastes employed in the study are possible precursors for making locally activated carbons at a low cost, thus resolving the problem of agro-waste disposal.

## 1. Introduction

Activated carbon AC, also commonly termed activated charcoal, has been defined differently by several authors as reported in the literature [1]. It is defined as a class of porous carbonaceous materials that can never be characterized by a structural formula or chemical analysis [2]. Further, AC can also be defined as a tasteless, solid, microcrystalline, nongraphitic form of black carbonaceous material with a very porous structure [3, 4]. Furthermore, other investigators state that AC refers to a porous material derived from a feedstock containing carbon with millions of tiny pores between the carbon atoms that have been opened due to the activation process [5]. Therefore, in summary, AC refers to a class of black carbonaceous porous materials with a large surface area prepared through the carbonization of any material rich with elemental carbon.

Activated carbon is a versatile adsorbent due to its good adsorption characteristics. The adsorption characteristics of activated carbon depend on the precursor type, size of the particles, and method adopted during preparation [6, 7].

The adsorbing quality of the resulting activated carbon is also influenced by the activating reagents, activation time, impregnation ratio, carbonization temperature, and the presence of inorganic impurities, among others [1]. The preparation of AC can be accomplished in two processes: physical and chemical. Physical activation involves carbonization of the precursor followed by the activation using different gases. At first, the material is carbonized at an elevated temperature of around 500–900°C without air. Then, the activation step, also termed oxidation, occurs when the material is exposed to an oxidizing environment, carbon dioxide, oxygen, or steam, at high temperatures ranging from 800 to 1000°C. Carbonization is purposely carried out to eliminate noncarbon elements from the raw materials, while the activation stage ensures that the desired porosity of the material is attained successfully [5].

Chemical activation, also known as the single-step method for the preparation of AC, occurs in the presence of activating chemical agents. Chemical activation has several advantages; first, it usually requires low activation temperature and shorter times for activation of the materials;

second, it can promote pore development in the carbon structure due to the effect of the chemicals. Generally, the carbon yields obtained by chemical activation are higher than those by physical activation. However, after thermal treatment, it needs a thorough process that recovers the chemical agents. This result might limit its usage due to environmental issues [8].

In general, activated carbon is prepared from materials rich in element carbon [9]. Two critical sources for activated carbon preparations are coal and agricultural wastes or biomass rich in lignocellulosic materials. The precursors used to prepare commercial activated carbons are highly costly and nonrenewable such as petroleum residues, lignite, wood, coal, and peat [1]. On the other hand, low-cost activated carbon is reported to have been successfully prepared from agricultural byproducts, for instance, Marula nutshell [10], grains, corn cobs, almond shells [11], and bamboo [10, 11].

Malawi is an agro-based developing country that generates large volumes of postharvest wastes every year through intensive farming. The wastes produced create a disposal challenge, contrary to developed countries where the agro-wastes become raw materials for various purposes in industrial applications. In Malawi, the tale is different; the wastes are dumped and burned in an open field resulting in the generation of greenhouse gases like carbon dioxide gases ( $\text{CO}_2$ ) that cause air pollution. In some urban and rural areas, the wastes are dumped in water sources, causing water pollution, and if the wastes are disposed of on land, it releases methane ( $\text{CH}_4$ ) gases due to the decomposition of organic matter, causing air and land pollution altogether. The practice used in the management of agro-waste results in environmental issues, and sometimes, the wastes act as vectors for disease-causing organisms, thereby threatening the public's health.

Various published articles mentioned agro-wastes such as rice husks and potato peels as raw materials for synthesizing low-cost activated carbons [12–15, 16]. However, most of these published papers have used sweet potato peels rather than Irish potato peels as precursors for synthesis of activated carbon and there is currently no published study that reports the fixed carbon content of the raw materials used to our knowledge. Furthermore, rice husks are known to be rich sources of silicates. In this current study, before rice husks were used in the preparation of activated carbon sodium silicate, an essential ingredient with wide industrial application in the manufacturing process was extracted.

In prior research, we showed that agro-wastes such as rice husks, *Jatropha curcas*, and cassava peels might be utilized to clarify wastewater and successfully eliminate turbidity and microbiological load from sewage wastewater collected at the Chikanda Wastewater Treatment Plant in Zomba city [17]. As a result, this effort focuses on increasing the value of diverse solid agro-wastes produced in Malawi.

Therefore, in this study, agro-wastes from Irish potato peels and rice husks after successful extraction of sodium silicate from rice husks were selected and used to prepare activated carbon by chemical activation as a way of sustainable waste management. Using these agro-wastes as AC precursors has substantial economic and environmental impacts

as converting undesirable agricultural waste to high-value adsorbents. Furthermore, using agro-waste residues as precursors for AC synthesis will also assist in our country's economic growth as it will reduce the importation of activated carbon from international markets.

## 2. Materials and Methods

**2.1. Materials and Reagents.** To synthesize activated carbon,  $\text{H}_3\text{PO}_4$ , NaOH, KI, and  $\text{NaSiO}_4$  were obtained from UNICHEM Reagent Co., while  $\text{KNO}_3$  was obtained from Lab-Chem, whereas HCl and  $\text{HNO}_3$  were sourced from DAEJUNG Co. and gasoline was purchased from the Total filling station. All reagents used were of analytical grade. Required solutions were made by dissolving the corresponding reagent in double-distilled water.

**2.2. Preparation of Activated Carbons.** Activated carbons were prepared through a chemical activation process according to the procedure by [18]. 100 g of rice husk fine powder was first soaked in 200 mL of 3  $\text{Mol}\cdot\text{L}^{-1}$  sodium hydroxide (NaOH) and left in an oven at a temperature of 105°C for 5 h. NaOH reacted with silica in rice husk powder producing soluble sodium silicate ( $\text{Na}_2\text{SiO}_3$ ). After that, the raw materials treated as solid base residues were washed with deionized water several times until the supernatant pH was neutral (pH = 7), oven dried at 110°C for 24 h, and used in the synthesis of activated carbon.

10 g of the dried solid residues and Irish potato peel powders were impregnated with 40% orthophosphoric acid ( $\text{H}_3\text{PO}_4$ ) ratios (1:1, 1:1.7, 1:2.5, and 1:3). The impregnated residues were left in an oven at 100°C for 12 h to reduce surplus water, and the dried samples were used for activation heated from room temperature. The samples were activated at different activation temperatures (400, 500, 600, and 700°C) with a constant activation time of 1.5 h. The samples were then cooled in desiccators and sequentially washed with 0.1 M NaOH, warm water, and finally cold water using the Buchner funnel until neutral pH was attained and then oven dried at a temperature of 105°C for 3 h. Finally, the samples were grounded, sieved with mesh 250  $\mu\text{m}$ , and stored in labeled plastic bottles waiting for characterization.

### 2.3. Characterization of Activated Carbon

**2.3.1. Determination of Activated Carbon Yield.** The weight of the precursors and activated carbons produced was measured using Mettler electronic balance. The carbon yield of each sample prepared was determined according to the procedure [19]. The carbon yield was calculated as

$$Y = \frac{W_f}{W_0} \times 100, \quad (1)$$

where  $Y$  is the carbon yield,  $W_f$  is the final weight of activated carbon recorded at the end of carbonization, and  $W_0$  is the initial weight of the impregnated precursors.

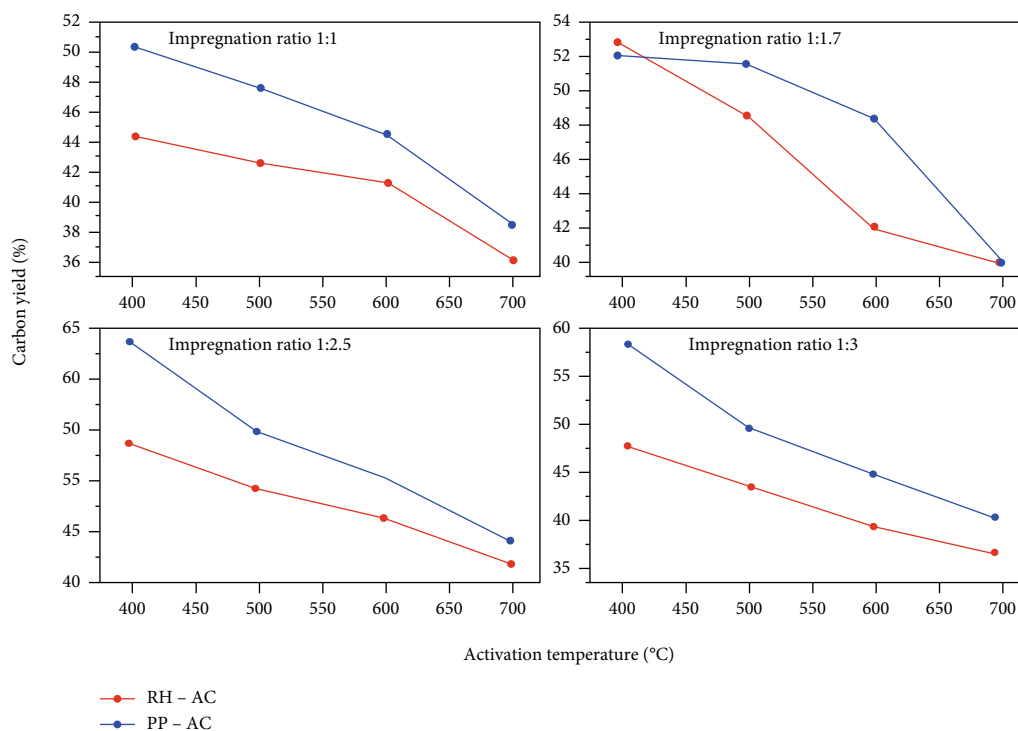


FIGURE 1: The effect of the impregnation ratio and carbonization temperature on carbon yield.

TABLE 1: The effect of the impregnation ratio and activation temperature on moisture content.

Impregnation Ratio	Activation temperature (°C)							
	400		500		600		700	
	RH-AC	PP-AC	RH-AC	PP-AC	RH-AC	PP-AC	RH-AC	PP-AC
1:1	3.65 ± 0.25	6.80 ± 0.2	4.9 ± 0.35	6.2 ± 0.40	4.4 ± 0.35	5.9 ± 0.25	4.4 ± 0.03	5.4 ± 0.3
1:1.7	3.45 ± 0.15	5.40 ± 0.1	4.5 ± 0.15	5.7 ± 0.15	3.7 ± 0.37	5.6 ± 0.15	4.2 ± 0.15	4.95 ± 0.15
1:2.5	3.15 ± 0.25	4.88 ± 0.32	4.4 ± 0.30	5.0 ± 0.20	4.2 ± 0.3	5.2 ± 0.2	4.1 ± 0.1	4.35 ± 0.25
1:3	2.95 ± 0.15	3.16 ± 0.34	4.1 ± 0.18	4.4 ± 0.24	3.6 ± 0.2	5.1 ± 0.2	4.05 ± 0.2	4.3 ± 0.2

2.3.2. *Determination of the Ash Content.* The ash content percentage was carried out [20] by a silica crucible preheated in the furnace at 900°C for 1 h. Then, it was cooled in a desiccator and reweighed. Next, 1 g of the AC sample was placed in a crucible covered with the lid and heated at 900°C for 1 h. The crucible and its content were then cooled in the desiccator and reweighed. The weight of the incombustible residues accounts for the ash content in the activated carbon samples. The ash content percentage was calculated using the equation given below:

$$\text{Ash content (\%)} = \frac{C - D}{C - B} \times 100, \quad (2)$$

where  $B$  is the weight of the crucible,  $g$ ,  $C$  is the weight of the crucible with the sample,  $g$ , and  $D$  is the weight of the crucible after weight loss  $g$ .

2.3.3. *Determination of Volatile Matter.* The volatile matter in activated carbon samples was determined [20]. Thus, a

silica crucible was preheated at a temperature of 900°C in a muffle furnace for 10 min. After that, samples were cooled in a desiccator. Next, 1 g of the activated carbon sample was placed in preheated silica crucible covered with the lid and placed in a muffle furnace and heated at the temperature of 900°C for 10 min. Finally, the crucible and contents were removed and cooled in a desiccator. The weight loss accounts for the volatile matter. The volatile matter was calculated as percentage using the equation as follows:

$$\text{Volatile matter (\%)} = \frac{[100(B - F) - M(B - G)]}{(B - G)(100 - M)} \times 100, \quad (3)$$

where  $B$  is the mass of the crucible and sample before heating,  $g$ ;  $F$  is the mass of the crucible with AC sample after heating,  $g$ ;  $G$  is the mass of the crucible with lid; and  $M$  is the moisture content of the activated carbon samples determined above.

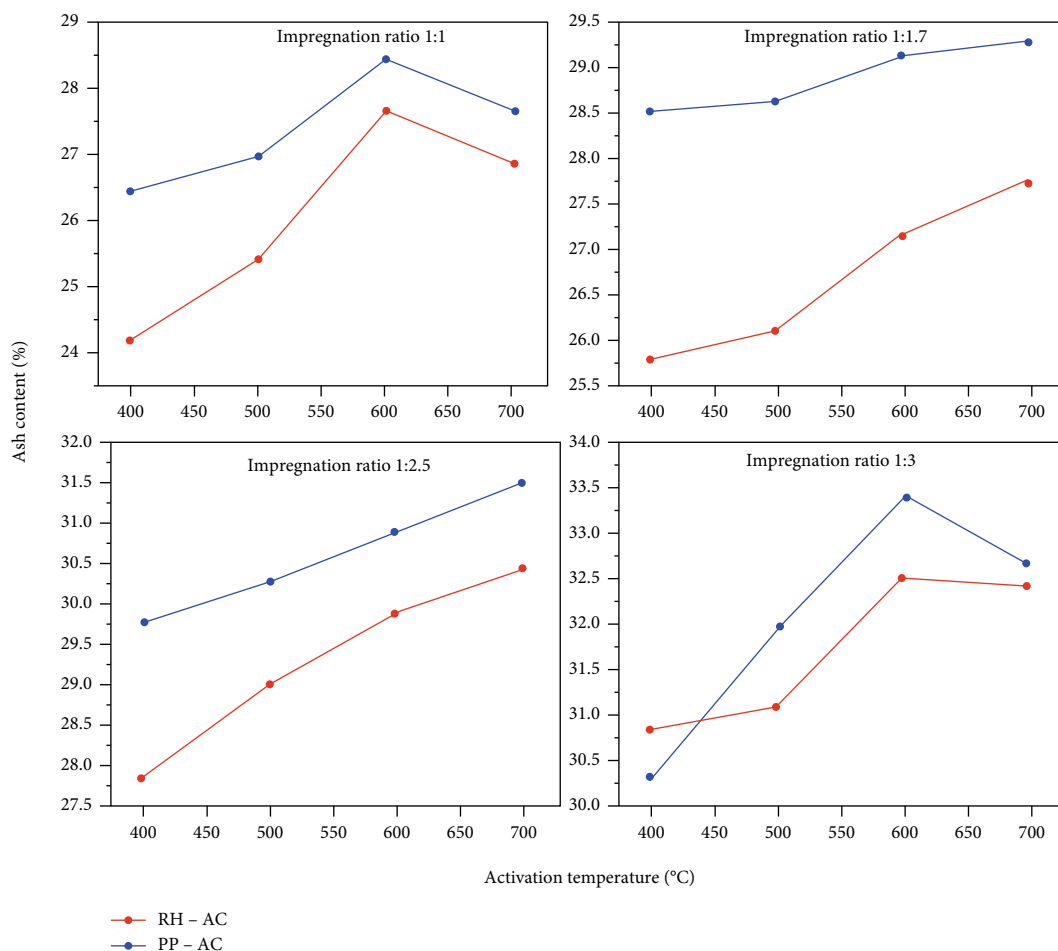


FIGURE 2: The effect of the impregnation ratio and activation temperature on the ash content.

**2.3.4. Determination of the Moisture Content.** The moisture content of the activated carbon samples was calculated according to [21], with some alterations in which 1 g of the activated carbon sample was weighed and placed in a porcelain cup. It was then oven heated at a temperature of 110°C for 3 h, cooled in a desiccator for 30 min, and reweighed. The weight change was measured as moisture lost and calculated as follows:

$$MC = \frac{B - C}{B - D} \times 100, \quad (4)$$

where MC is the moisture content,  $B$  is the weight of the porcelain plus the activated carbon sample,  $C$  is the weight of the porcelain plus the dried activated carbon sample, and  $D$  is the mass of empty porcelain.

**2.3.5. Determination of the Fixed Carbon Content.** The fixed carbon content in activated carbon samples was calculated as [22]. The equation which was involved in fixed carbon content calculation is given as

$$FCC = 100 - (\%M + \%A + \%VM), \quad (5)$$

where FCC is the fixed carbon content,  $\%M$  is the percentage of moisture contained in the activated carbon sample,

$\%A$ : is the percentage of ash contained in the activated carbon sample, and  $\%VM$ : is the percentage of volatile matter in the activated carbon sample.

**2.3.6. Determination of the Iodine Number.** All working solutions were prepared according to the American Society of Testing and Measurement [23]. Iodine number calculations followed the procedure described by [20].

$$\text{Iodine number} \left( \frac{\text{mg}}{\text{g}} \right) = \frac{(B - S)}{B} \times \frac{VM}{W} \times 253.81, \quad (6)$$

where  $B$  and  $S$  are the volumes of the thiosulfate solution required for blank and sample titrations, respectively;  $W$  is the weight of the activated carbon sample;  $M$  is the concentration (Mol) of iodine solute, 253.81 g/Mol = molar weight iodine; and  $V$  is the volume (mL) of aliquot.

**2.3.7. Determination of Ammonia and Gasoline Adsorption.** In gas-phase applications, activated carbon samples were evaluated in gasoline and ammonia (25%  $\text{NH}_3$ ) adsorption. The procedure used was similar for both gasoline and ammonia adsorption. Thus, 0.5 g of AC samples was weighed using Mettler electronic balance and transferred into crucibles whose initial mass was recorded previously.

TABLE 2: The volatile matter in the prepared activated carbon samples.

Impregnation	Activation temperature (°C)							
	400		500		600		700	
Ratio	RH-AC	PP-AC	RH-AC	PP-AC	RH-AC	PP-AC	RH-AC	PP-AC
1:1	14.05 ± 0.17	16.22 ± 0.24	12.79 ± 0.33	15.02 ± 0.04	12.34 ± 0.13	14.39 ± 0.07	12.89 ± 0.02	12.38 ± 0.15
1:1.7	15.33 ± 0.11	16.37 ± 0.62	13.09 ± 0.32	15.07 ± 0.09	13.34 ± 0.36	14.88 ± 0.11	13.28 ± 0.31	12.48 ± 0.26
1:2.5	17.61 ± 0.18	18.12 ± 0.35	14.35 ± 0.14	16.52 ± 0.18	14.43 ± 0.25	15.51 ± 0.17	14.09 ± 0.32	14.01 ± 0.12
1:3	18.01 ± 0.13	18.66 ± 0.19	15.39 ± 0.17	16.76 ± 0.13	14.58 ± 0.32	15.61 ± 0.15	14.58 ± 0.20	14.51 ± 0.17

TABLE 3: The fixed carbon content of the prepared activated carbons.

Impregnation	Activation temperature (°C)							
	400		500		600		700	
Ratio	RH-AC	PP-AC	RH-AC	PP-AC	RH-AC	PP-AC	RH-AC	PP-AC
1:1	57.48 ± 0.69	49.88 ± 0.21	55.88 ± 0.35	49.39 ± 0.29	54.49 ± 0.39	49.88 ± 0.39	53.27 ± 0.31	50.79 ± 0.25
1:1.7	56.21 ± 0.32	48.16 ± 0.27	55.46 ± 0.79	49.28 ± 0.12	51.96 ± 0.63	47.99 ± 0.42	50.88 ± 0.22	49.78 ± 0.35
1:2.5	52.07 ± 0.18	46.68 ± 0.01	52.97 ± 0.52	45.58 ± 0.22	50.99 ± 0.25	47.90 ± 0.13	44.78 ± 0.56	48.10 ± 0.42
1:3	51.4 ± 0.51	44.47 ± 0.50	51.33 ± 0.56	46.45 ± 1.31	47.08 ± 0.20	47.08 ± 0.20	44.76 ± 0.20	47.68 ± 0.46

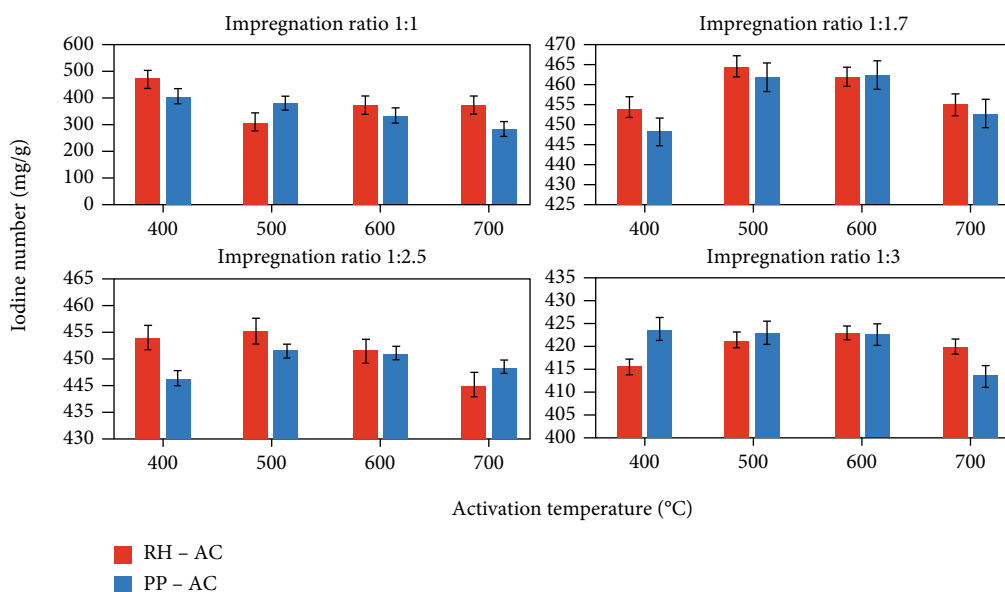


FIGURE 3: The iodine number of the prepared activated carbon samples.

Then, the samples were then taken into desiccators and sealed together with either ammonia or gasoline. The samples were left for 24 h in desiccators for adsorption to occur. After 24 h, AC samples were also reweighed and the change in mass was assumed due to the gas absorbed by the samples. Finally, the adsorption percentage was calculated using the equation reported previously by [5].

$$\text{Adsorption (\%)} = \frac{\Delta m}{M_b} \times 100, \quad (7)$$

where  $\Delta m$  is the change in mass of activated carbon after gas adsorption and  $M_b$  is the mass of activated carbon before gas adsorption.

**2.3.8. Adsorbent Characterization.** The surface charge of the adsorbents was determined by pH titration [24–26]. The 50 mL volume of 0.01 M  $\text{KNO}_3$  was sealed in a volumetric flask containing 50 mg of the adsorbents under different pH conditions. The pH of the solutions was adjusted by drop-wise addition of 0.1 M NaOH or 0.1 M HCl solutions until the desired pH was achieved. The suspensions of

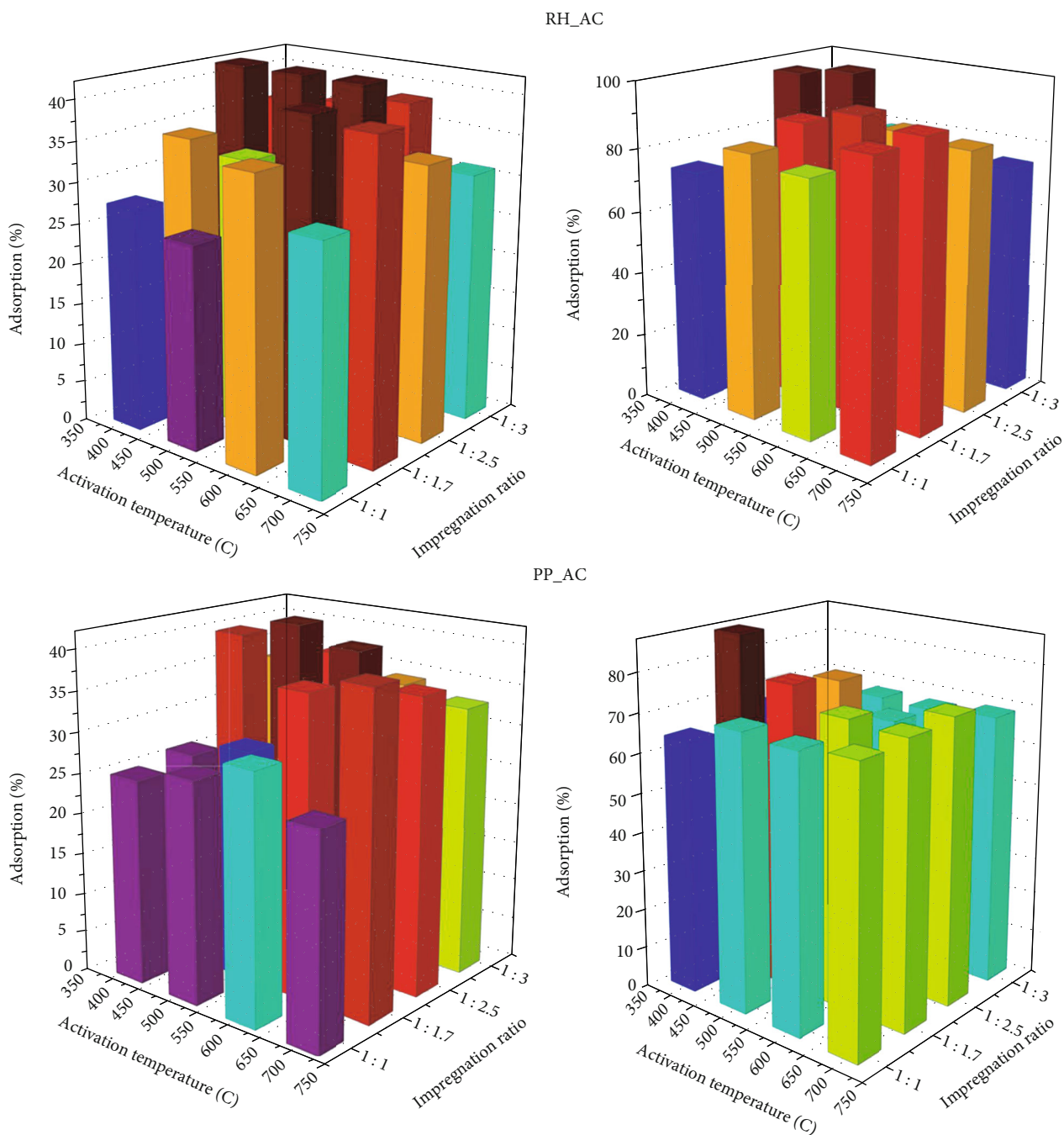


FIGURE 4: Ammonia (a) and gasoline (b) adsorption of the prepared activated carbons.

activated carbons in the flasks were then agitated for 48 h. The plot between initial pH versus the change in pH was plotted, and the point of intersection was considered the point of charge. Surface chemistry was determined using FT-IR Spectroscopy (NICOLET iS 10, 2007, USA). The ratio of 1 : 10 mg thus KBr to adsorbent was adopted. The samples were analyzed, and the spectra were recorded in the range 4000 to 400  $\text{cm}^{-1}$ . The crystallinity analysis was carried out by Siemens X-ray diffractometer (model no: 10190376, Germany). The scan runs were performed at a diffraction angle of ( $2\theta$ ) with a variation ranging between 10° and 90°. The

surface morphology of the adsorbents was carried out by FESEM (JEOL JSM-7100F, Japan).

### 3. Results and Discussions

#### 3.1. Physicochemical Properties

**3.1.1. Carbon Yield.** The carbon yield results for the prepared RH-AC and PP-AC show that as activation temperature increases from 400°C to 700°C at impregnation ratios 1:1 to 1:3; the percentage of carbon yield decreases as presented

in Figure 1. The results showed that increasing carbonization temperature decreases the percentage of AC yield. This result is likely associated with promoting carbon burn-off and volatilization of tar at elevated temperatures. Again, the decrease in carbon yield could be attributed to the increasing impregnation ratio, which promotes the release of volatiles from the sample resulting in the decrease in carbon yield. The lower carbon yield with a higher impregnation ratio might be due to the enhancement of carbon burn-off by excess activating agents [27, 28]. A similar pattern of results was reported in the literature by investigators who worked on deriving activated carbon from agro-wastes [29]. Higher carbon yield on prepared carbons was attained in PP-AC samples than RH-AC.

**3.1.2. Moisture Content.** The moisture content in prepared activated carbon was determined to ascertain its suitability in adsorption studies. The results indicate an increase in impregnation ratios from 1:1 to 1:3 and carbonization temperature from 400°C to 700°C for both RH-AC and PP-AC; the moisture content of the derived activated carbon samples reduced as shown in Table 1. It was observed that as the activation temperature increased, the moisture content in activated carbon samples decreased. This result might be connected to removing volatile matter, thereby reducing carbon yield and concurrently reducing the moisture content in the prepared RH-AC and PP-AC samples. The samples with a similar impregnation ratio but different activation temperatures had minimal moisture content. The activated carbon derived from potato peels had high moisture content instead of activated carbon obtained from rice husks. The comparison of prepared activated carbons with commercial activated carbon was made, and the results displayed by RH-AC were similar to that of commercial activated charcoal (4%).

**3.1.3. Ash Content.** The ash content findings are presented in Figure 2. The results showed that increasing impregnation ratios from 1:1 to 1:3 and carbonization temperature from 400 to 700°C for both RH-AC and PP-AC increased the ash content for both the prepared RH-AC and PP-AC samples. It was noted that increasing the activation temperature increased the ash content in activated carbon samples. The increase in ash content might be associated with a high degree of biomass burn-off at elevated temperatures. Comparing the ash content with commercial activated carbon, the ash content in all prepared activated charcoal samples exceeded the recommended range of 2–10 (%) but activated carbon prepared from rice husks had less ash content. This result implies that the activated carbons synthesized were not of high purity. However, different investigators reported similar results in the literature on activated carbons from agro-wastes [30].

**3.1.4. Volatile Matter.** While the impregnation ratio increases from 1:1 to 1:3 with activation temperature from 400°C to 700°C, volatile matter decreases for RH-AC and PP-AC (Table 2). The results indicated that increasing carbonization temperature caused a decrease in the volatile matter content in both RH-AC and PP-AC. The reduction

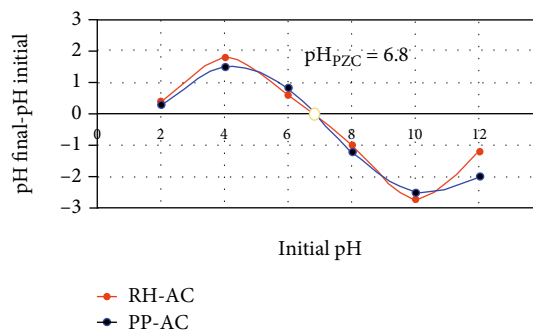


FIGURE 5: The point of zero charge plot for RH-AC and PP-AC.

in the volatile matter percentage as activation temperature increases is connected to the fact that more volatile matter is released at an elevated temperature, lowering its content in activated carbon samples. The study has recognized high-volatile matter content in activated carbon samples prepared from Irish potato peels compared with rice husks. Volatile matter in commercial activated carbon was noted at 30% compared to prepared activated carbon samples within the required range.

**3.1.5. Fixed Carbon Content.** The carbon content in prepared activated carbon samples was calculated. At given impregnation ratios 1:1 to 1:3 and increasing carbonization temperature from 400°C to 700°C, the carbon content for the prepared activated carbon samples decreased as displayed in Table 3. The fixed carbon content results depend on volatile matter, ash, and moisture content. The results indicated that an increase in carbonization temperatures promotes the release of volatile matter and increases the ash content while at the same time decreasing the moisture content. The activated carbons prepared at 400°C were within the recommended range of commercial activated carbon, whereas in commercial activated carbon, the carbon content ranges 50–95%. The activated carbon derived from rice husks had carbon content within the commercial activated charcoal.

**3.1.6. Iodine Number.** The iodine number of the prepared activated carbons was calculated. Results shown in Figure 3 indicate that as carbonization temperature changed from 400°C to 700°C with an impregnation ratio from 1:1 to 1:1.7, the value of the iodine number also increased. However, the further increase of impregnation to 1:3 resulted in reduction in the iodine number, as presented in Figure 3. So, as impregnation increases, the decrease in iodine number might be associated with the excess dehydration and destruction of micropores at a higher impregnation ratio. If the micropores are destroyed to form larger pores, the iodine number and adsorption capacity eventually decrease [2–16, 24–26, 31–35]. According to the findings, it can be observed that the prepared activated carbons gave a higher iodine number of 420 mg/g than commercial activated carbon. On the other hand, the activated carbon prepared from rice husks produced a higher iodine value than activated carbon prepared from potato peels.

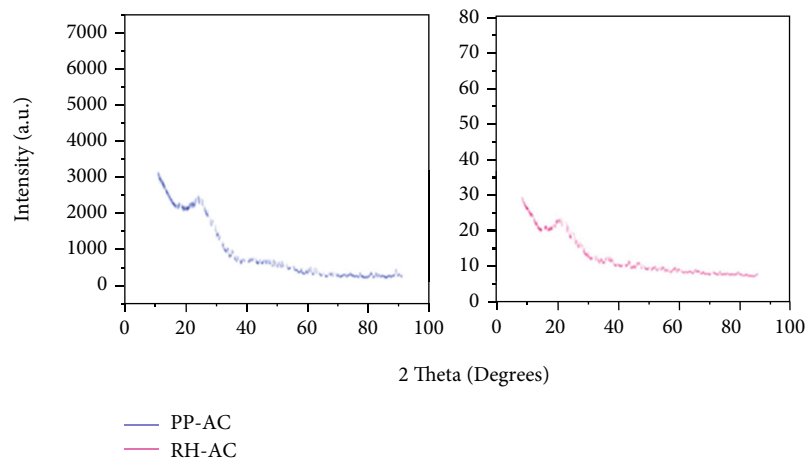


FIGURE 6: The XRD spectra for RH-AC and PP-AC, respectively.

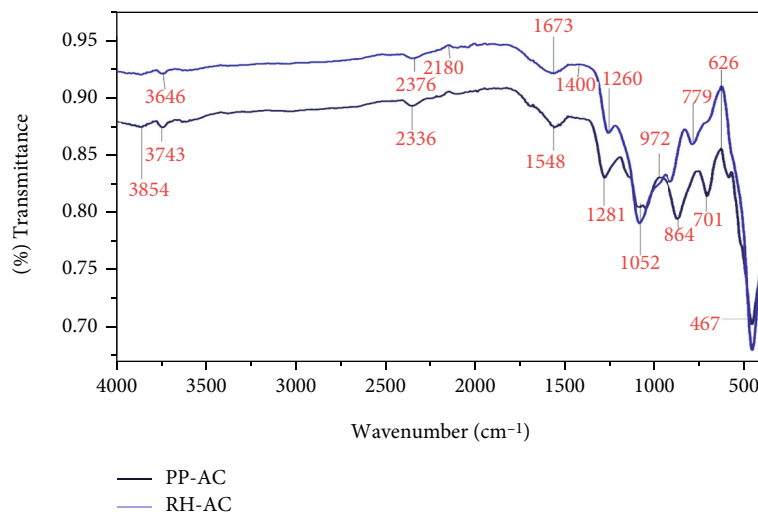
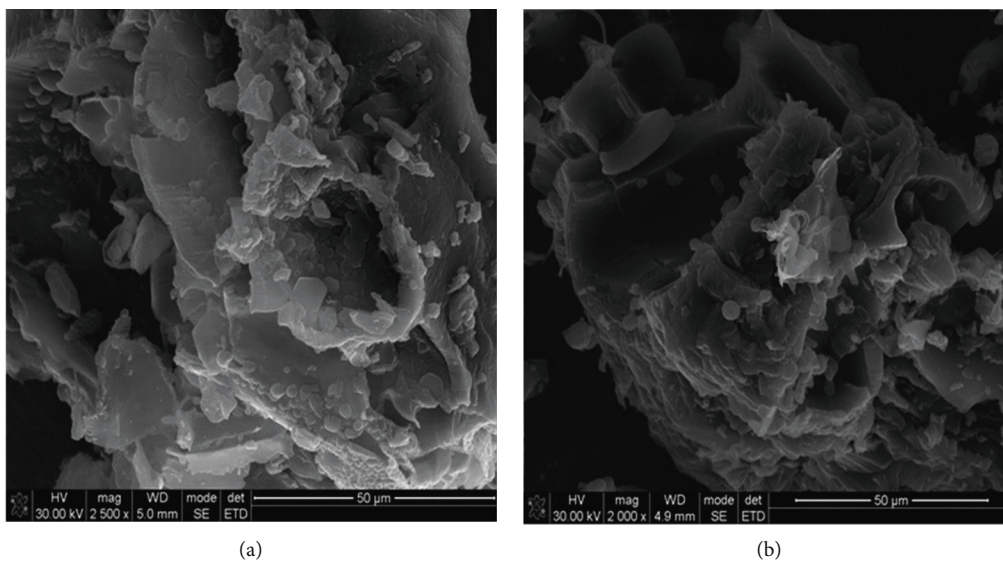


FIGURE 7: The IR spectra for RH-AC and PP-AC, respectively.



(a)

(b)

FIGURE 8: FESEM micrographs (a) PP-AC and (b) RH-AC.



TABLE 4: A comparison of the characteristics of the activated carbons with other literature reported values.

Precursor	Activator	Activation temp ( $^{\circ}\text{C}$ )	Functional groups	XRD	SEM	pHpzc	Reference
<i>Wisteria sinensis</i> seeds	KOH	850	C=O, C=C, O-H, C-O	Amorphous	Mesoporous surface	—	[42]
Biomass date seeds	$\text{H}_2\text{SO}_4$ , KOH	600–900	O-H, C=O, C-O	—	—	—	[43]
Coffee grounds	KOH	800	C=O, O-H, C-O	—	Microporous surface	—	[44]
Tobacco cigarettes	$\text{ZnCl}_2$	700	C=C, CH, OH	—	Microporous surface	7.47	[45]
NaOH	700	C=C, C=N, OH	—	Mesoporous surface	12.84	—	[45]
Tobacco stems	$\text{H}_3\text{PO}_4$	750	OH, C-O, C=O, C-C	—	Mesoporous surface	9.59	[46]
<i>Acacia auriculiformis</i>	$\text{H}_3\text{PO}_4$	850	—	—	Microporous surface	4.8	[47]
NaOH	850	—	—	Mesoporous surface	8.2	—	[47]
NaCl	850	—	—	Microporous surface	6.8	—	[47]
Almond shell	$\text{H}_3\text{PO}_4$	600	$\text{COO}^-$ , C=O, C-H,	—	Microporous surface	5.5	[48]
Pineapple wastes	$\text{ZnCl}_2$	500	OH, N-O, C-N	—	Mesoporous surface	—	[49]
Baobab fruit shells	$\text{H}_3\text{PO}_4$	700	C=C, C-O, C-H	Amorphous	Microporous surface	—	[41]
Food wastes	$\text{ZnCl}_2$	500–600	C-O, C=C, C=O, O-H	Amorphous	Mesoporous surface	—	[50]
<i>Lemnaminor</i>	$\text{H}_3\text{PO}_4$	600	N-H, C-H, O-H, C=O	—	Mesoporous surface	—	[51]
<i>Daniellia oliveri</i>	$\text{H}_3\text{PO}_4$	—	OH, C-H, $\text{C}\equiv\text{C}$ , C=C	—	Microporous surface	7.6	[52]
<i>Leucaena leucocephala</i>	NaOH	550	C=O, $\text{C}\equiv\text{C}$ -H, C=C, OH	—	Mesoporous surface	5.2	[53]
Rice husk	NaOH	650	—	Amorphous	Mesoporous surface	—	[54]
Hazelnut husk	—	950	—	Amorphous	Microporous surface	—	[55]
Green vegetable wastes	KOH	800	$\text{C}\equiv\text{N}$ , C=O, CH, OH	—	Microporous surface	—	[56]
Soya bean straw	NaOH	120	CH, C-O, OH	—	Mesoporous surface	—	[57]
Feather fiber	—	600	N-C=O, C-C, C-N	—	Mesoporous surface	5.94	[58]
Human hair	—	500	C=O, C=C, C-OH, C-H	Amorphous	Microporous surface	—	[59]
Mango kernel	$\text{H}_3\text{PO}_4$	600	N-H, C=O, OH, CH	—	Mesoporous surface	6.8	[60]
Rice husks	$\text{H}_3\text{PO}_4$	500	C=O, OH, C-O, $\text{C}\equiv\text{C}$	Amorphous	Microporous surface	6.8	This study
Irish potato peels	$\text{H}_3\text{PO}_4$	500	$\text{C}\equiv\text{C}$ , C=O, C-O, OH	Amorphous	Microporous surface	6.8	This study

**3.1.7. Ammonia and Gasoline Adsorption.** The results for ammonia and gasoline adsorption are presented in Figure 4. Results showed that at impregnation ratios from 1:1 to 1:3 and as carbonization temperature increased from 400°C to 700°C, the adsorption rates of gasoline and ammonia firstly increased and, a few moments after, started to decrease. These results might be connected with heat treatment during carbonization, facilitating pore opening and widening and increasing the surface area. However, massive thermal treatment results in carbon burn-off affecting the pore size and surface area of the activated carbon, affecting adsorbing capacities [14, 16]. The lowest values in ammonia gas and gasoline adsorption efficiency were attained in activated carbon samples derived from potato peels compared to rice husk activated charcoal.

**3.2. Point of Zero Charges ( $pH_{pzc}$ ).** The point of zero charge(s) for the prepared activated carbons was evaluated through a 0.01 M  $KNO_3$  solution. The pH adjustment was performed by drop-wise addition of either 0.1 M NaOH or 0.1 M HCl.  $pH_{pzc}$  is used to evaluate the pH of the adsorbents. Figure 5 shows the results of RH-AC and PP-AC having a similar point of zero charges equivalent to  $pH_{pzc} = 6.8$ . At this point, the adsorbents have a net electrical neutral charge on the surface. When the solution pH is lower than the  $pH_{pzc}$ , the adsorbent surface becomes protonated due to excess competition of  $H^+$  ions resulting in the surface favoring the removal property of contaminants like anions. When pH is greater than the  $pH_{pzc}$ , the adsorbent surface becomes deprotonated by  $OH^-$  ions in the solution and the surface has a negative charge density and favors the adsorption of pollutants like cations [36]. The prepared activated carbon  $pH_{pzc}$  was nearby neutral pH.

**3.3. X-Ray Diffractions.** The X-ray pattern of the prepared activated carbons is presented in Figure 6. The results show the Bragg diffraction peak for both activated carbon samples at the region of  $2\theta = 20-30^\circ$ . The existence of the hump depicts the high degree of disorder characteristic of carbonaceous materials. Furthermore, the nonappearance of a sharp peak suggests that no discrete mineral peaks were noticed in the samples [37]. Similar patterns were also reported by other researchers who prepared activated carbons from agro-wastes [19, 20].

**3.4. Surface Functional Group Results.** The results for functional groups of the activated carbon understudy are shown in Figure 7. The peaks observed at wavenumbers, 3743–3646  $cm^{-1}$ , are assigned to the stretching bond vibration of free hydrogen bonded to  $^-OH$  groups [38]. The absorption bands at around 2336–2376  $cm^{-1}$  are associated with stretching vibration of the C-O for carbon dioxide or carbon monoxide derivatives. The peak present at 2180  $cm^{-1}$  corresponds to bond stretching vibrations of alkynes ( $C\equiv C$ ). The bands visible at (1673, 1400)  $cm^{-1}$  relate to the stretching vibration of  $C=C$  in the benzene ring [39]. The N-oxide group observed at 1548  $cm^{-1}$  was assigned to asymmetric and symmetric stretching ( $N=O$ ). The peak detected at 1052  $cm^{-1}$  is associated with the antisymmetric stretch of

C-O-C [40]. The presence of the most functional groups indicates suitable characteristics of the activated carbons.

**3.5. FESEM Results.** The micrographs shown in Figure 8 revealed a porous surface area accompanied by several wide opening pores of different sizes and shapes. The images revealed cavities, porous structures, and large interconnected pores that allow access to inner zones of the adsorbents. The chemical activation of precursors at 500°C with 40% orthophosphoric acid ( $H_3PO_4$ ) resulted in an extensive removal of volatile matter and promoted the opening and formation of more pores (micropores and mesopores) on the surface of the adsorbents [41]. The pre-existent pores had a crucial role in increasing the surface area of the prepared carbon. The results suggest that the prepared adsorbents could be suitable for various uses due to the surface porosity.

The characteristic results of the prepared activated carbons were compared with other adsorbents. Table 4 provides the key features of derived activated carbon compared to other adsorbents mentioned in the literature.

## 4. Conclusion

The study has shown that the activated carbons prepared were not of high purity due to, among other factors, high ash content, moisture content, and less fixed carbon content as compared to commercial activated carbon. Nevertheless, the iodine value was much higher than that of commercial activated carbon. Furthermore, the analysis has confirmed that the prepared activated carbons were amorphous with the small crystalline domain, more porous, and with surface functional groups appearing at fingerprint regions. The study has further demonstrated that the materials understudy could be viable raw materials to prepare low-cost but high-porous activated carbon for adsorbing chemical pollutants in water and wastewater treatment. This result also offers a solution to the challenges Malawi as a developing country faces in agro-waste disposal.

## Data Availability

All data are included within the article.

## Conflicts of Interest

The authors declare that there are no conflicts of interest.

## Acknowledgments

The authors gratefully acknowledge the assistance rendered by professor Wellington Masamba of Botswana International University of Science and Technology for using the instruments for sample characterization.

## References

- [1] A. YAhya, Z. Al-qodah, and C. W. Z. Ngah, "Agricultural bio-waste materials as potential sustainable precursors used for activated carbon production: A review," *Renewable and Sustainable Energy Reviews*, vol. 46, pp. 218–235, 2015.

- [2] P. Prabu and K. Raghu, "Synthesis and characterization of cotton stalk activated carbon by chemical activation using  $H_3PO_4$ ," *Journal of Advanced Science and Research*, vol. 2, no. 5, pp. 93–97, 2017.
- [3] P. Ravichandran, P. Sugumaran, S. Seshadri, and A. Basta, *Optimizing the Route for Production of Activated Carbon from Casuarina Equisetifolia Fruit Waste*, Royal Society of Chemistry, 2018.
- [4] M. A. Yahya, M. H. Mansor, W. Amani, and A. Wan, "A brief review on activated carbon derived from agriculture by-product," in *In AIP Conference Proceedings*, AIP Publishing LLC, 2018.
- [5] J. Ahnemark and S. Marques, *Preparation of Activated Carbon from Caribbean Pine by Chemical Activation*, Royal Institute of Technology, Department of Chemical Engineering, 2013.
- [6] R. Chen, L. Li, Z. Liu et al., "Preparation and characterization of activated carbons from tobacco stem by chemical activation," *Air & waste*, vol. 67, no. 6, pp. 713–724, 2017.
- [7] M. D. F. Salgado, A. M. Abioye, and M. Mat, "Preparation of activated carbon from babassu endocarp under microwave radiation by physical activation," *Earth Environment Science*, vol. 105, p. 012116, 2018.
- [8] C. Grima-olmedo, Á. Ramírez-gómez, D. Gómez-limón, and C. Clemente-jul, "Activated carbon from flash pyrolysis of eucalyptus residue," *Heliyon*, vol. 2, no. 9, p. e00155, 2016.
- [9] M. S. Shamsuddin, N. R. N. Yusoff, and M. A. Sulaiman, "Synthesis and characterization of activated carbon produced from kenaf core fiber using  $H_3PO_4$  activation," *Procedia Chemistry*, vol. 19, pp. 558–565, 2016.
- [10] T. Mkungunugwa, S. Manhokwe, A. Chawafambira, and M. Shumba, "Synthesis and characterisation of activated carbon obtained from Marula (*Sclerocarya birrea*) nutshell," *Journal of Chemistry*, vol. 2021, 9 pages, 2021.
- [11] S. Hosseini, S. Masoudi Soltani, H. Jahangirian, F. Eghbali Babadi, T. S. Y. Choong, and N. Khodapanah, "Fabrication and characterization porous carbon rod-shaped from almond natural fibers for environmental applications," *Journal of Environmental Chemical Engineering*, vol. 3, no. 4, pp. 2273–2280, 2015.
- [12] R. Riyanto, B. I. Astuti, and B. I. Mukti, "Simple preparation of rice husk activated carbon (RHAC) and applications for laundry and methylene blue wastewater treatment," *AIP Conference Proceedings*, 2017, p. 20033, 2017.
- [13] A. H. Wazir, I. U. Wazir, and A. M. Wazir, "Preparation and characterization of rice husk based physical activated carbon," *Energy Sources, Part A Recovery. Utilisation Environmental Effects*, pp. 1–11, 2020.
- [14] L. Muniandy, F. Adam, A. R. Mohamed, and E. P. Ng, "The synthesis and characterization of high purity mixed microporous/mesoporous activated carbon from rice husk using chemical activation with NaOH and KOH," *Microporous Mesoporous Materials*, vol. 197, pp. 316–323, 2014.
- [15] M. Rhaman, M. Haque, M. Rouf, M. Siddique, and M. Islam, "Preparation and characterization of activated carbon & amorphous silica from rice husk," *Bangladesh Journal of Science and Industrial Research*, vol. 50, no. 4, pp. 263–270, 2015.
- [16] M. Bernardo, S. Rodrigues, N. Lapa et al., "High efficacy on diclofenac removal by activated carbon produced from potato peel waste," *International Journal of Environment Science and Technology*, vol. 13, no. 8, pp. 1989–2000, 2016.
- [17] J. B. Njewa, E. Vunain, and T. Biswick, "Wastewater clarification and microbial load reduction using agro- forestry and agricultural wastes," *Tanzania Journal of Science*, vol. 47, no. 1, pp. 19–33, 2021.
- [18] Y. Li, X. Zhang, R. Yang, G. Li, and C. Hu, "The role of  $H_3PO_4$  in the preparation of activated carbon from NaOH-treated rice husk residue," *Royal Society of Chemistry*, vol. 5, no. 41, pp. 32626–32636, 2015.
- [19] I. A. W. Tan, A. L. Ahmad, and B. H. Hameed, "Preparation of activated carbon from coconut husk: Optimization study on removal of 2,4,6-trichlorophenol using response surface methodology," *Journal of Hazardous Materials*, vol. 153, no. 1–2, pp. 709–717, 2008.
- [20] C. Pongener, D. Kibami, and R. Goswamee, "Synthesis and characterization of activated carbon from the biowaste of the plant *Manihot esculenta*," *Chemical Sciences Transactions*, vol. 1, no. 4, pp. 59–68, 2015.
- [21] A. S. Alzaydien, "Physical, chemical and adsorptive characteristics of local oak sawdust based activated carbons," *Asian Journal Scientific Research*, vol. 9, no. 2, pp. 45–56, 2016.
- [22] D. Kibami, C. Pongener, K. S. Rao, and S. Dipak, "Preparation and characterization of activated carbon from *Fagopyrum esculentum* Moench by  $HNO_3$  and  $H_3PO_4$  chemical activation," *Pelagia Research Library*, vol. 5, no. 4, pp. 46–55, 2014.
- [23] ASTM, "Standard Test Method for Determination of Iodine Number of Activated Carbon 1," *West Conshohocken, PA: American Society for Testing Materials*, vol. 94, pp. 1–5, 2006.
- [24] E. Scapin, G. P. S. Maciel, A. S. Polidoro et al., "Activated carbon from rice husk biochar with high surface area," *Biointerface Research in Applied Chemistry*, vol. 11, no. 3, pp. 10265–10277, 2020.
- [25] G. Z. Kyzas, E. A. Deliyanni, and K. A. Matis, "Activated carbons produced by pyrolysis of waste potato peels: cobalt ions removal by adsorption," *Colloids Surfaces A: Physicochemical Engineering Aspects*, vol. 490, pp. 74–83, 2016.
- [26] S. Liang and A. G. McDonald, "Chemical and thermal characterization of potato peel waste and its fermentation residue as potential resources for biofuel and bioproducts production," *Journal of Agriculture and Food Chemistry*, vol. 62, no. 33, pp. 8421–8429, 2014.
- [27] R. Gottipati, "Preparation and characterization of microporous activated carbon from biomass and its application in the removal of chromium (VI) from aqueous phase," in *Department of Chemical Engineering National Institute of Technology Rourkela*, Odisha, India, 2012.
- [28] K. Riahi, S. Chaabane, and B. Ben Thayer, "Marble wastes as amendments to stabilize heavy metals in Zn-electroplating sludge," *Advances in Environmental Research*, vol. 6, no. 1, pp. 15–23, 2017.
- [29] S. E. Abechi, C. E. Gimba, A. Uzairu, and Y. A. Dallatu, "Preparation and characterization of activated carbon from palm kernel shell by chemical activation," *Research Journal. Chemical Sciences*, vol. 3, no. 7, pp. 54–61, 2013.
- [30] B. O. Evbuomwan, A. S. Abutu, and C. P. Ezech, "The effects of carbonization temperature on some physicochemical properties of bamboo based activated carbon by potassium hydroxide (KOH) activation," *Journal of Physical Sciences*, vol. 3, pp. 187–191, 2012.
- [31] H. I. Adamu and J. D. Putshak, "Production and characterization of activated carbon from leather waste, sawdust, and lignite," *Chemsearch Journal*, vol. 1, no. 1, pp. 10–15, 2010.

- [32] M. Saadia, O. Nazha, A. Abdlemjid, and B. Ahmed, "Preparation and characterization of activated carbon from residues of oregano," *Journal of Surface Science Technology*, vol. 28, no. 3, pp. 91–100, 2012.
- [33] M. Ahiduzzaman and A. K. M. Sadrul Islam, "Preparation of porous bio-char and activated carbon from rice husk by leaching ash and chemical activation," *Springerplus*, vol. 5, no. 1, p. 1248, 2016.
- [34] A. I. Osman, J. Blewitt, J. Abu-Dahrieh et al., "Production and characterisation of activated carbon and carbon nanotubes from potato peel waste and their application in heavy metal removal," *Environment Science and Pollution Research*, vol. 26, no. 36, pp. 37228–37241, 2019.
- [35] D. Pertiwi, N. Yanti, and R. Taslim, "High potential of yellow potato (*Solanum Tuberosum* L.) peel waste as porous carbon source for supercapacitor electrodes," *Journal Physics Conference Series*, vol. 2193, no. 1, p. 012019, 2022.
- [36] D. Lataye, D. Malwade, V. Kurwadkar, S. Mhaisalkar, and D. Ramirez, "Adsorption of hexavalent chromium onto activated carbon derived from *Leucaena leucocephala* waste sawdust : kinetics, equilibrium and thermodynamics," *International journal of Environmental Science and Technology*, vol. 13, no. 9, pp. 2107–2116, 2016.
- [37] E. Vunain and T. Biswick, "Adsorptive removal of methylene blue from aqueous solution on activated carbon prepared from Malawian baobab fruit shell wastes : equilibrium , kinetics and thermodynamic studies and thermodynamic studies," *Separation Science Technology*, vol. 54, pp. 1–15, 2019.
- [38] N. S. Barot and H. K. Bagla, "Eco-friendly waste water treatment by cow dung powder ( adsorption studies of Cr (III), Cr (VI) and Cd (II) using tracer technique)," *Desalination and Water Treatment*, vol. 38, no. 1–3, pp. 104–113, 2012.
- [39] T. Benzaoui, A. Selatnia, and D. Djabali, "Adsorption of copper (II) ions from aqueous solution using bottom ash of expired drugs incineration," *Adsorption Science and Technology*, vol. 36, no. 1-2, pp. 114–129, 2018.
- [40] R. Labied, O. Benturki, A. Hamitouche, and A. Donnot, "Adsorption of hexavalent chromium by activated carbon obtained from a waste lignocellulosic material (*Ziziphus jujubacores*): kinetic, equilibrium, and thermodynamic study," *Adsorption Science and Technology*, vol. 36, no. 3-4, pp. 1066–1099, 2018.
- [41] E. Vunain, D. Kenneth, and T. Biswick, "Synthesis and characterization of low-cost activated carbon prepared from Malawian baobab fruit shells by  $H_3PO_4$  activation for removal of cu(II) ions: equilibrium and kinetics studies," *Applied Water Science*, vol. 7, no. 8, pp. 4301–4319, 2017.
- [42] G. P. Awasthi, D. P. Bhattarai, B. Maharjan, K. S. Kim, C. H. Park, and C. S. Kim, "Synthesis and characterizations of activated carbon from *Wisteria sinensis* seeds biomass for energy storage applications," *Journal of Industrial Engineering Chemistry*, vol. 72, pp. 265–272, 2019.
- [43] A. E. Ogungbenro, D. V. Quang, K. A. Al-Ali, L. F. Vega, and M. R. M. Abu-Zahra, "Synthesis and characterization of activated carbon from biomass date seeds for carbon dioxide adsorption," *Journal of Environmental Chemical Engineering*, vol. 8, no. 5, article 104257, 2020.
- [44] H. Laksaci, A. Khelifi, M. Trari, and A. Addoun, "Synthesis and characterization of microporous activated carbon from coffee grounds using potassium hydroxides," *Journal of Cleaner Production*, vol. 147, pp. 254–262, 2017.
- [45] E. Conradi, A. C. Gonçalves, D. Schwantes et al., "Development of renewable adsorbent from cigarettes for lead removal from water," *Journal Environmental Chemical Engineering*, vol. 7, no. 4, p. 103200, 2019.
- [46] J. Manfrin, A. C. Gonçalves, D. Schwantes, C. R. T. Tarley, A. D. P. Schiller, and G. J. Klassen, "Triple activation (thermal-chemical-physical) in the development of an activated carbon from tobacco: characterizations and optimal conditions for  $Cd^{2+}$  and  $Pb^{2+}$  removal from waters," *Water Practice and Technology*, vol. 15, no. 4, pp. 877–898, 2020.
- [47] D. O. Kra, N. B. Allou, P. Atheba, P. Drogui, and A. Trokourey, "Preparation and Characterization of Activated Carbon Based on Wood (*Acacia auriculaeformis*, Côte d'Ivoire)," *Journal of Encapsulation Adsorption Sciences*, vol. 9, no. 2, pp. 63–82, 2019.
- [48] B. N. Rai, B. S. Giri, Y. Nath et al., "Adsorption of hexavalent chromium from aqueous solution by activated carbon prepared from almond shell: kinetics, equilibrium and thermodynamics study," *Journal of Water Supply Research and Technology*, vol. 67, no. 8, pp. 724–737, 2018.
- [49] K. N. Mahmuda, T. H. Wen, and Z. A. Zakaria, "Activated carbon and biochar from pineapple waste biomass for the removal of methylene blue," *Environmental Toxicology Management*, vol. 1, no. 1, pp. 30–36, 2021.
- [50] A. Santhosh and S. S. Dawn, "Synthesis of zinc chloride activated eco-friendly nano-adsorbent (activated carbon) from food waste for removal of pollutant from biodiesel wash water," *Water Science and Technology*, vol. 84, no. 5, pp. 1170–1181, 2021.
- [51] Y. Huang, S. Li, H. Lin, and J. Chen, "Fabrication and characterization of mesoporous activated carbon from *Lemna minor* using one-step  $H_3PO_4$  activation for Pb(II) removal," *Applied Surface Science*, vol. 317, pp. 422–431, 2014.
- [52] G. B. A. H. I. Adegoke and S. Fauzeeyat, "Adsorption of Cr (VI) ions onto goethite, activated carbon and their composite : kinetic and thermodynamic studies," *Applied Water Science*, vol. 10, no. 9, pp. 1–18, 2020.
- [53] A. S. Yusuff, "Adsorption of hexavalent chromium from aqueous solution by *Leucaena leucocephala* seed pod activated carbon: equilibrium, kinetic and thermodynamic studies," *Arab Journal of Basic and Applied Sciences*, vol. 26, no. 1, pp. 89–102, 2019.
- [54] A. Mullick, S. Moulik, and S. Bhattacharjee, "Removal of hexavalent chromium from aqueous solutions by low-cost rice husk-based activated carbon : kinetic and thermodynamic studies," *Indian Chemical Engineering*, vol. 60, no. 1, pp. 1–14, 2018.
- [55] D. D. Milenković, M. M. Milosavljević, A. D. Marinković, V. R. Dokić, J. Z. Mitrović, and A. L. J. Bojić, "Removal of copper(II) ion from aqueous solution by high-porosity activated carbon," *Water SA*, vol. 39, no. 4, pp. 515–522, 2013.
- [56] M. I. Sabela, K. Kunene, S. Kanchi et al., "Removal of copper (II) from wastewater using green vegetable waste derived activated carbon: an approach to equilibrium and kinetic study," *Arabian Journal of Chemistry*, vol. 12, no. 8, pp. 4331–4339, 2019.
- [57] B. Zhu, T. Fan, and D. Zhang, "Adsorption of copper ions from aqueous solution by citric acid modified soybean straw," *Journal of Hazardous Materials*, vol. 153, no. 1–2, pp. 300–308, 2008.
- [58] P. Benjwal, R. Sharma, and K. K. Kar, "Effects of surface microstructure and chemical state of featherfiber-derived multidoped

- carbon fibers on the adsorption of organic water pollutants,” *Materials and Design*, vol. 110, pp. 762–774, 2016.
- [59] R. Kumar, S. Varshney, K. K. Kar, and K. Dasgupta, “Enhanced thermo-mechanical and electrical properties of carbon-carbon composites using human hair derived carbon powder as reinforcing filler,” *Advanced Powder Technology*, vol. 29, no. 6, pp. 1417–1432, 2018.
- [60] M. K. Rai, G. Shashi, V. Meena, S. Chakraborty, R. S. Singh, and B. N. Rai, “Removal of hexavalent chromium Cr (VI) using activated carbon prepared from mango kernel activated with  $H_3PO_4$ ,” *Resource-Efficient Technology*, vol. 2, pp. S63–S70, 2016.